

AD-A077 684

SPECTROLAB INC SYLMAR CALIF  
LOW RESISTIVITY-HIGH MINORITY CARRIER LIFETIME SINGLE CRYSTAL S--ETC(U)  
APR 79 P M STELLA , R W OPJORDEN

F/G 20/2

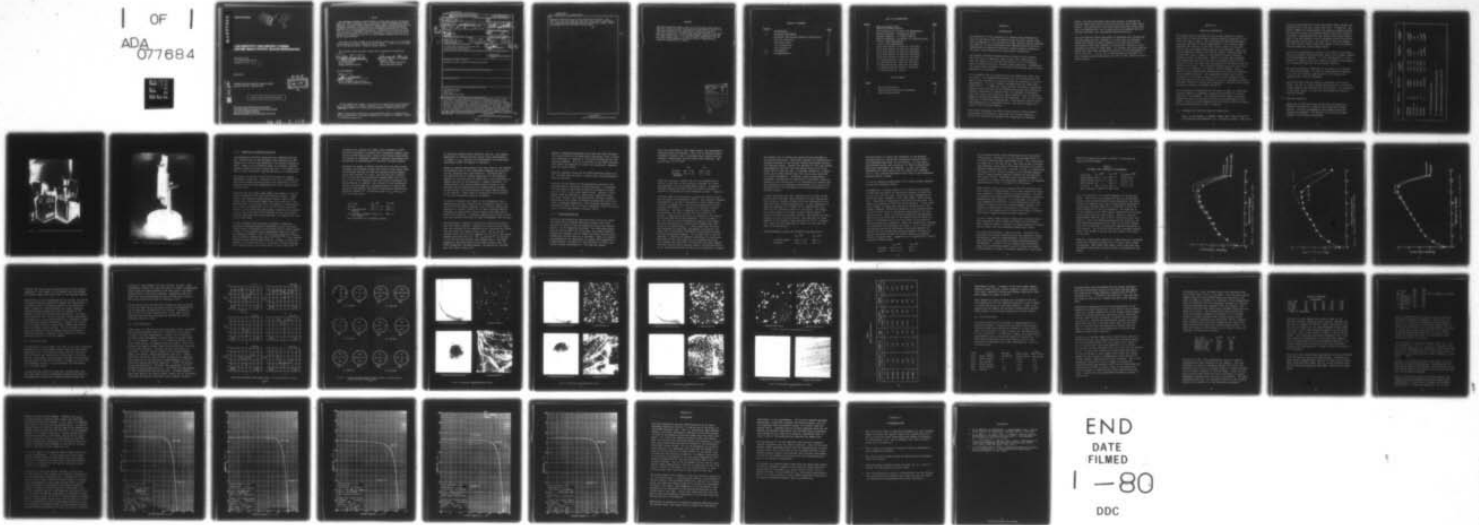
F33615-77-C-2045

AFAPL-TR-79-2031

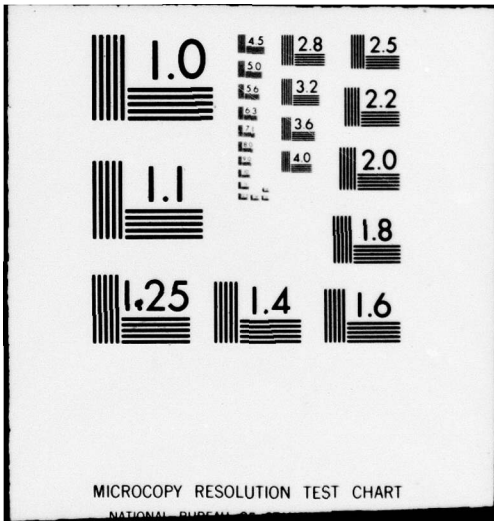
NL

UNCLASSIFIED

| OF |  
ADA  
677684



END  
DATE  
FILMED  
1-80  
DDC



AD A 077684

AFAPL-TR-79-2031

LEVEL <sup>II</sup>

# LOW RESISTIVITY-HIGH MINORITY CARRIER LIFETIME SINGLE CRYSTAL SILICON INVESTIGATION

SPECTROLAB, INC.  
12500 GLADSTONE AVENUE  
SYLMAR, CA 91342

330 250

APRIL 1979

INTERIM TECHNICAL REPORT AFAPL-TR-79-2031  
Report for July 1977 - September 1978

DDC  
RECEIVED  
DEC 6 1979  
A

DDC FILE COPY

Approved for public release; distribution unlimited.

AIR FORCE AERO PROPULSION LABORATORY  
AIR FORCE WRIGHT AERONAUTICAL LABORATORIES  
AIR FORCE SYSTEMS COMMAND  
WRIGHT-PATTERSON AIR FORCE BASE, OHIO 45433

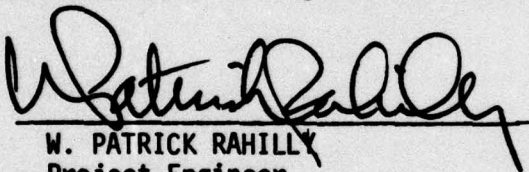
79 22 5 018

NOTICE

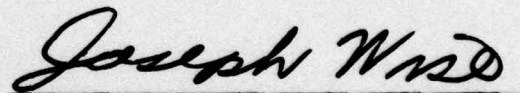
When Government drawings, specifications, or other data are used for any purpose other than in connection with a definitely related Government procurement operation, the United States Government thereby incurs no responsibility nor any obligation whatsoever; and the fact that the government may have formulated, furnished, or in any way supplied the said drawings, specifications, or other data, is not to be regarded by implication or otherwise as in any manner licensing the holder or any other person or corporation, or conveying any rights or permission to manufacture, use, or sell any patented invention that may in any way be related thereto.

This report has been reviewed by the Information Office (OI) and is releasable to the National Technical Information Service (NTIS). At NTIS, it will be available to the general public, including foreign nations.

This technical report has been reviewed and is approved for publication.



W. PATRICK RAHILLY  
Project Engineer  
Energy Conversion Branch



JOSEPH F. WISE  
TAM, Solar Energy Conversion  
Energy Conversion Branch

FOR THE COMMANDER



JAMES D. REAMS  
Chief, Aerospace Power Division  
Air Force Aero Propulsion Laboratory

"If your address has changed, if you wish to be removed from our mailing list, or if the addressee is no longer employed by your organization please notify AEAPL/POE-2, W-PAFB, OH 45433 to help us maintain a current mailing list".

Copies of this report should not be returned unless return is required by security considerations, contractual obligations, or notice on a specific document.

UNCLASSIFIED

SECURITY CLASSIFICATION OF THIS PAGE (When Date Entered)

REPORT DOCUMENTATION PAGE		READ INSTRUCTIONS BEFORE COMPLETING FORM
1. REPORT NUMBER <b>18</b> AFAP/ TR-79-2031	2. GOVT ACCESSION NO.	3. RECIPIENT'S CATALOG NUMBER <b>9</b>
4. TITLE (and Subtitle) <b>6</b> LOW RESISTIVITY - HIGH MINORITY CARRIER LIFETIME SINGLE CRYSTAL SILICON INVESTIGATION	5. TYPE OF REPORT & PERIOD COVERED Interim Technical Report Jul 77 - Sep 78	
6. AUTHOR(s) <b>10</b> Paul → M. Stella R. W. Opjorden	7. CONTRACT OR GRANT NUMBER(s) <b>15</b> F33615-77-C-2045	
8. PERFORMING ORGANIZATION NAME AND ADDRESS Spectrolab, Inc. T2500 Gladstone Avenue Sylmar CA 91342 <i>Subcontract</i>	9. PROGRAM ELEMENT, PROJECT, TASK AREA & WORK UNIT NUMBERS <b>16</b> 2308-S3-01 <b>17</b> 53	10. REPORT DATE <b>11</b> Apr 79 <b>12</b> 50
11. CONTROLLING OFFICE NAME AND ADDRESS Air Force Aero Propulsion Laboratory (POE) Wright-Patterson AFB OH 45433	13. SECURITY CLASS. (of this report) UNCLASSIFIED	
14. MONITORING AGENCY NAME & ADDRESS (if different from Controlling Office) 61102F	15a. DECLASSIFICATION/DOWNGRADING SCHEDULE	
16. DISTRIBUTION STATEMENT (of this Report) Approved for public release; distribution unlimited.		
17. DISTRIBUTION STATEMENT (of the abstract entered in Block 20, if different from Report)		
18. SUPPLEMENTARY NOTES		
19. KEY WORDS (Continue on reverse side if necessary and identify by block number) Silicon Solar Cells High Purity Silicon Solar Cells Space Photovoltaic Power		
20. ABSTRACT (Continue on reverse side if necessary and identify by block number) The objective of this program is to improve the performance of N+/P silicon solar cells by improving the minority carrier lifetime of moderate to low resistivity silicon material. The behavior of cells fabricated from improved material will be demonstrated by measuring electrical output without irradiation and after 1 Mev electrons and 10 Mev proton irradiation. This report discusses the first fifteen months' efforts toward developing and evaluating a new solar cell silicon material. During this time period, equipment and techniques for material growth have been developed along with analysis of methods for removing		

DD FORM 1 JAN 73 1473

EDITION OF 1 NOV 65 IS OBSOLETE

UNCLASSIFIED

SECURITY CLASSIFICATION OF THIS PAGE (When Date Entered)

330 250

st

UNCLASSIFIED

SECURITY CLASSIFICATION OF THIS PAGE(When Data Entered)

impurities from non-ultra pure silicon after wafer fabrication. Five preliminary ultra pure ingots have been grown using boron ion implantation and a single ingot using elemental gallium to provide the P dopant. Results are presented for solar cells made from the ingots.

UNCLASSIFIED

SECURITY CLASSIFICATION OF THIS PAGE(When Data Entered)

FOREWORD

This Interim Technical Report covers all work performed under Contract F33615-77-C-2045, entitled, "Low Resistivity-High Minority Carrier Lifetime Single Crystal Silicon Investigation", during the period of July 1977 to Sept 1978. The effort was sponsored by the Air Force Aero Propulsion Laboratory, Air Force Systems Command, Wright-Patterson AFB Ohio under Project 3145. Dr W. Patrick Rahilly (AFAPL/POE-2) was the Air Force Project Engineer, and Mr Paul Stella of Spectrolab was technically responsible for the work.

Accession For	
NTIS GRA&I	<input checked="" type="checkbox"/>
DDC TAB	<input type="checkbox"/>
Unannounced	<input type="checkbox"/>
Justification	
By _____	
Distribution/	
Availability Codes	
Dist	Avail and/or special
A	

LIST OF ILLUSTRATIONS

Page

TABLE OF CONTENTS

Page

Section

Page

I	INTRODUCTION	1
II	TECHNICAL DISCUSSION	3
	Equipment and Starting Material Acquisition	3
	Impurity Gettering	4
	Delivered Ingots	20
	Ingot Evaluation	21
	Cell Evaluation	29
III	CONCLUSIONS	40
IV	RECOMMENDATIONS	42

LIST OF TABLES

Page

Page

1	Solid Concentration	1
2	Delivered Cell Electrical Performance	2
3	Ingots Characteristics	3

## LIST OF ILLUSTRATIONS

<u>Figure</u>		<u>Page</u>
1	Modified Siemens VZA-3 Float Zone Crystal Grower	6
2	Ingot Holding Jig for Boron Ion Implantation	7
3	Spectral Response - Phosphorous Getter	17
4	Spectral Response - Al (evap.) Getter	18
5	Spectral Response - Al Getter (0.5 ohm-cm silicon)	19
6	2-Point Probe Measurements	22
7	4-Point Probe Measurements	23
8	Sirtl Etch Pattern of Ingot No. F01774703	24
9	Sirtl Etch Pattern of Ingot No. F01774701	25
10	Sirtl Etch Pattern of Ingot No. F02774201	26
11	Sirtl Etch Pattern of Ingot No. F01774503	27
12	Sirtl Etch Pattern of Ingot No. F01775001	27
13	I-V Characteristics, Ingot No. F01774703	35
14	I-V Characteristics, Ingot No. F01774202	36
15	I-V Characteristics, Ingot No. F01774503	37
16	I-V Characteristics, Ingot No. F01775001	38
17	I-V Characteristics, Control	39

## LIST OF TABLES

<u>Table</u>		<u>Page</u>
1	Doping Concentration	5
2	Gettered Cell Electrical Performance	16
3	Ingot Characteristics	28

## SECTION I

### INTRODUCTION

The objective of this program is to improve the performance of N+/P silicon solar cells by improving the minority carrier lifetime of moderate to low resistivity single crystal silicon material. The behavior of cells fabricated from improved material will be demonstrated by measuring electrical output without irradiation and after 1 MeV electron and 10 MeV proton irradiation.

The primary difference between material used in this contract and that which is generally used in solar cell fabrication is that the improved silicon starting material is of the highest purity available with only residual boron remaining. Furthermore, the ingot growth technique is by vacuum float zoning which provides additional purification.

It is proposed that by elimination of all impurities, other than the dopant, the recombination centers will be eliminated and the open circuit voltage will increase toward the theoretical value of approximately 0.7 volts, thereby increasing the cell efficiency dramatically. In addition, since electron and proton irradiation creates vacancies which in turn migrate until they are captured by chemical impurities or interstitials, the removal of impurities from the silicon could allow for rapid removal of the irradiation damage by preventing trapping of the vacancies. This in turn would eliminate a significant contribution to the minority carrier lifetime degradation in irradiated silicon, and lead to higher cell output during a flight mission.

This report discusses the first fifteen month's efforts toward developing and evaluating a new solar cell silicon material. During this time period equipment and techniques for material

growth have been developed along with analysis of methods for removing impurities from non-ultra pure silicon after wafer fabrication. Five preliminary ultra pure ingots have been grown using boron ion implantation and a single one using elemental gallium additive and solar cells evaluated from the materials.

The boron implant wafers have shown no advantage over conventional crucible grown silicon, although it is felt that the technique rather than method of ingot formation is at fault due to the occurrence of very high numbers of dislocations, leading to polycrystalline sections in some cases. In contrast the single gallium doped ingot has shown considerable promise with the achievement of 633 mV (at 25°C)  $V_{oc}$  on the 0.2 ohm-cm material and short circuit currents ninety eight percent of that of the 2 ohm-cm crucible grown controls.

## SECTION II

### TECHNICAL DISCUSSION

The primary dopant selected for the silicon crystals is boron, since this is also the primary residual impurity remaining in the float zone grown ingots. The two methods of boron doping which have been selected are boron implantation (to be done at Hughes Research Labs, Malibu, California) using a boron tri-fluoride source ( $\text{BF}_3$ ) and gaseous boron doping, using diborane ( $\text{B}_2\text{H}_6$ ) gas. The ion-implanted ingots will then be regrown (recrystallized) by vacuum float zone in order to distribute the boron uniformly through the bulk of the ingot. Boron in silicon has a segregation coefficient near unity so that the sweeping effect of the molten zone does not alter the distribution of the boron along the length of the ingot. The projected resistivities are for p-type material at 0.2 ohm-cm, 2.0 ohm-cm, and 20.0 ohm-cm. Table 1 shows the calculated doping concentrations for both the implanted and the diborane doping. The implantation energy was 100 Kev. In addition to the boron implant using  $\text{B}^+$  ions, implantation was also planned using the  $\text{BF}_2^+$  species in order to determine possible favorable effects of the fluorine impurity on resultant cell characteristics, notably the leakage current.<sup>(1)</sup>

Gallium doping was scheduled for one ingot in order to investigate reported radiation resistance properties attributed to silicon doped with this element. The superior lattice match of gallium compared to boron in silicon is certainly one advantage of this dopant. (Doping is with elemental Ga in the seed transition region.) The projected resistivity was 0.2 ohm-cm.

#### 2.1 Equipment and Starting Material Acquisition

Early in the program, a Siemen's model VZA-3 soner (Figure 1) was purchased from Westech, Inc. of Phoenix Arizona. This unit,

originally designated for float zone growth under vacuum, was modified with a new tank circuit and coil. In addition, the growth chamber was made suitable for positive pressure growth. An argon gas control and diborane doping system was likewise installed. Considerable care was given to providing cleanliness in the gas system by use of stainless steel fittings and spectroscopic purity gas. The plan was to use this furnace for final single crystal float-zone growth of the ion-implant, diborane doped and gallium doped ingots.

For the ion implantation, a special jig (Figure 2) was fabricated for holding the pre-purified ingots in the sample chamber of the implantation machine. In this configuration, it was possible to implant one entire side of an ingot by overlapping the 2" beam exit aperture of the implant machine.

The pre-purification ingots were to be grown in an existing 1" float zone furnace. In order to guard against contamination, the oil diffusion pump system on this furnace was replaced with a new CTI-Cryopump.

The poly silicon starting material consisted of two basic types. For use in initial growth setup studies, 4-7K ohm-cm p-type material was acquired from Dow Corning. For the growth of the final ingots, 4.2 kgm of 9.20K ohm-cm was obtained from Dow Corning.

## 2.2 Impurity Gettering

Gettering of impurities from silicon was considered as a possible alternative to growing ultra high purity doped silicon. The use of phosphorous and aluminum gettering sources was examined. The results of this work are described in the following paragraphs.

TABLE 1  
DOPING CONCENTRATION

<u>Crystal #</u>	<u>Dopant (1)</u>	<u>Dopant Method</u>	<u>Ave. Resist.</u> $\Omega\text{-cm}$ Calcul. Meas.	<u>Dopant Conc.</u> $\text{cm}^{-3}$	<u>Donor Conc.</u> $\text{cm}^{-3}$
F01774503	B	Implant.	0.20 0.19	$2.3 \times 10^{17}$	$2.0 \times 10^{13}$
F01774202	B	Implant.	2.00 2.90	$8.7 \times 10^{15}$	$2.7 \times 10^{13}$
F02774201 (2)	$\text{BF}_2$	Implant.	2.00 7.20	NA	NA
F01774703	B	Implant.	20.00 23.60	NA	NA
F01774701	B	Implant.	20.00 24.80	$6.3 \times 10^{14}$	$1.2 \times 10^{13}$
F01775001	Ga	Doped Seed	0.20 0.25	$2.3 \times 10^{17}$ (3)	$0.9 \times 10^{12}$

(1) All final doped ingots are p-type

(2) The implanted ion species was  $\text{BF}_2$  rather than B

(3) Residual boron concentration was  $2.0 \times 10^{13} \text{ cm}^{-3}$

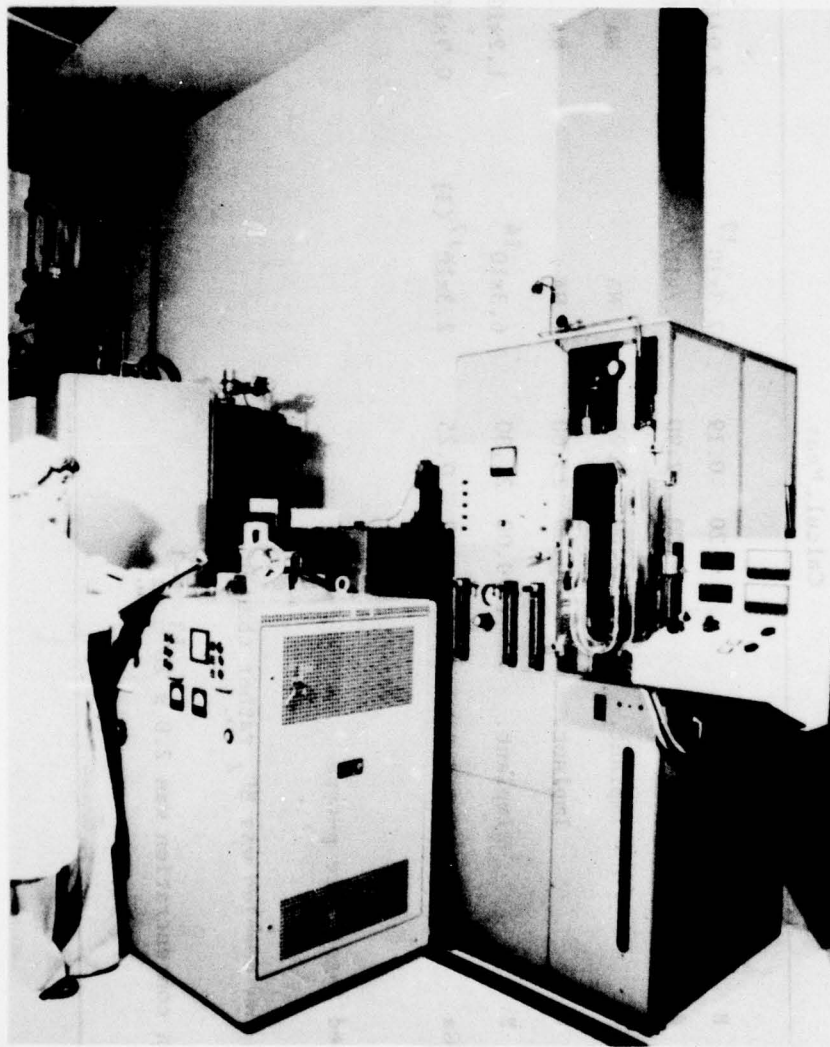


Figure 1 Modified Siemens VZA-3 Float Zone Crystal Grower

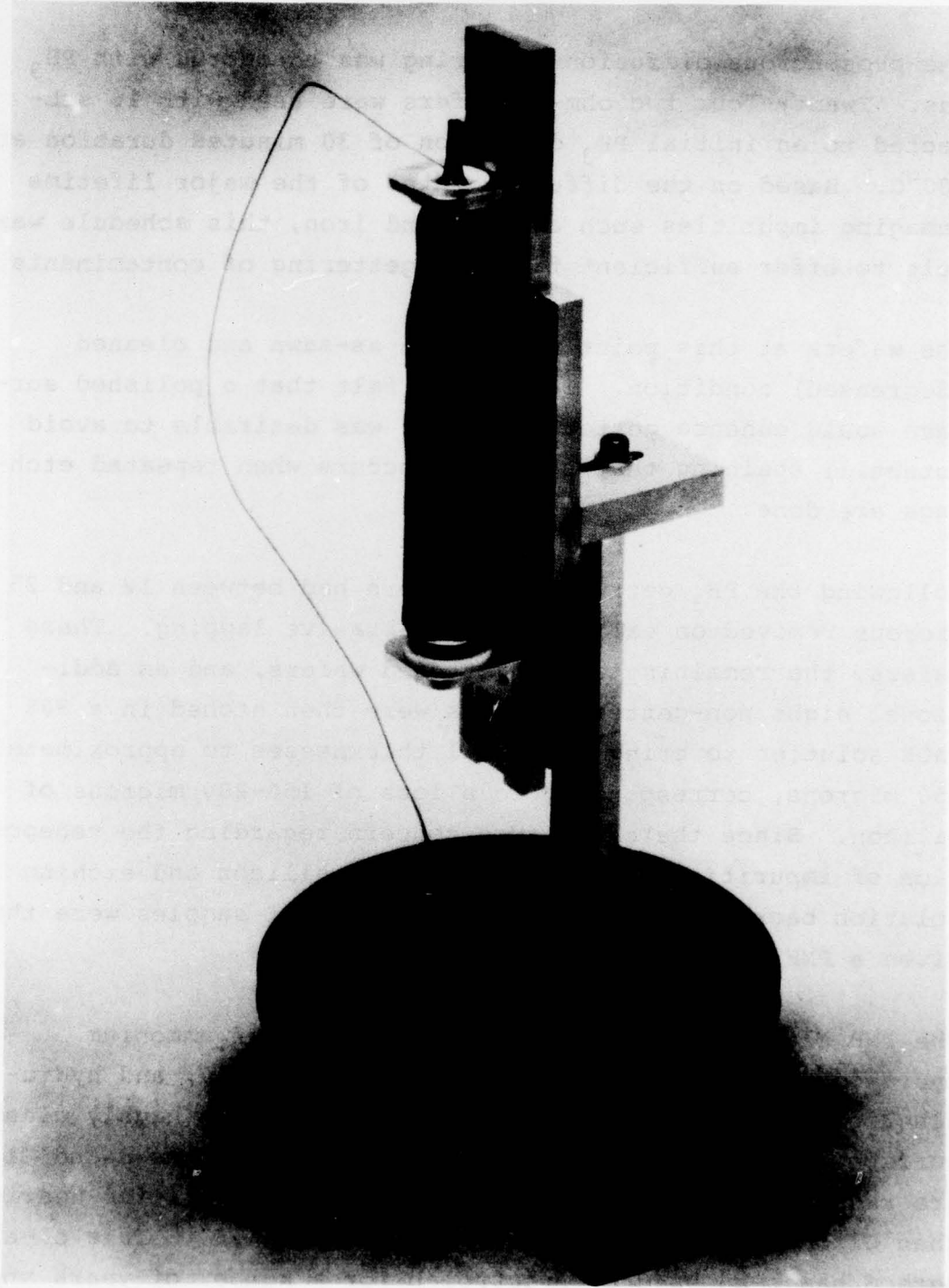


Figure 2 Ingot Holding Jig For Boron Ion Implantation

### 2.2.1 Phosphorous Diffusion Gettering

The phosphorous diffusion gettering was conducted with  $\text{PH}_3$  gas. Twenty-four two ohm-cm wafers were used with 16 subjected to an initial  $\text{PH}_3$  diffusion of 30 minutes duration at  $900^\circ\text{C}$ . Based on the diffusion rates of the major lifetime damaging impurities such as gold and iron, this schedule was felt to offer sufficient time for gettering of contaminants.

The wafers at this point were in an as-sawn and cleaned (degreased) condition. It was not felt that a polished surface would enhance gettering and it was desirable to avoid potential staining that sometimes occurs when repeated etchings are done.

Following the  $\text{PH}_3$  getter eight wafers had between 12 and 25 microns removed on each side with abrasive lapping. These wafers, the remaining eight gettered wafers, and an additional eight non-gettered wafers were then etched in a 30% NaOH solution to bring the final thicknesses to approximately 250 microns, corresponding to a loss of 150-200 microns of silicon. Since there was some concern regarding the redeposition of impurities from the etched-off silicon and etching solution back onto the silicon surface, all samples were then given a PNH clean.

The PNH cleaning technique uses a sequence of ammonium hydroxide, hydrogen peroxide, hydrochloric acid, and hydrofluoric acid, to provide a silicon wafer with a highly cleaned surface. It is reported that contaminants such as S and Cl are reduced to levels  $\sim 10^{13} \text{ cm}^{-2}$  and that impurities heavier than Cl occur at levels well below  $10^{12} \text{ cm}^{-2}$ .<sup>(2)</sup> This cleaning method has been used by Spectrolab for a number of years and proved to be quite effective in minimizing lifetime degradation occurring during the fabrication of boron BSF cells.<sup>(3)</sup>

Following the cleaning all wafers were diffused at 825°C and then subjected to standard cell processing stopping just before the AR coating step, since an AR coating would affect the results of subsequent spectral response measurements and complicate the determination of any bulk lifetime effects.

Although all groups of wafers started with the same initial thickness the diffused surface was found to etch faster than non-diffused surfaces so that the gettered-and-not-lapped cells were thinnest at 9 mils, the controls were thickest at 11.9 mils and the gettered and lapped wafers were 10.5 mils, the 1.4 mil reduction from the control case being the amount removed in lapping. As a result of the differences corrections were made for thickness based on in-house work partially published in the Twelfth Photovoltaic Specialists Conference Record.<sup>(4)</sup> Corrected values of  $I_{sc}$  and  $V_{oc}$  at 25°C are shown below:

Cell Type	$I_{sc}$ (mA)	$V_{oc}$ (mV)
Control	104.2 ± 1.9	584 ± 3
PH <sub>3</sub> Gettered and* Etched	101.1 ± 1.6	588 ± 5
PH <sub>3</sub> Gettered, lapped* and etched	102.5 ± 1.3	585 ± 4

\*data corrected for thickness effects

Following the cleaning all wafers were diffused at 825°C  
No gettering benefits were observed, with all cell groups comparable in voltage and the control cells approximately 2% higher in  $I_{sc}$ , although all measurements are essentially equivalent within the degree of accuracy.

Spectral response measurements were then taken on the samples. A noticeable loss in long wavelength response was found for the  $PH_3$  gettered cells (see Figure 3). Although some of this might be due to lifetime impairment in the gettered samples, it was felt that at least half of the difference in samples was due to the variation in sample thickness. As stated earlier the control samples were thickest at 300 microns, and the gettered and not-lapped wafers thinnest at 225 microns, and the gettered and lapped samples midway at 260 microns. These relative differences were reflected in the long wavelength spectral responses.

In order to minimize the impact of any degradation due to temperature, the  $PH_3$  gettering was re-examined using a one half hour 850°C getter sequence. The 2 ohm-cm samples were prepared in a manner similar to the 900°C gettered samples, although the post getter silicon removal used NaOH etching without any lapping. In addition samples were etched so that test and control cells were of equal thicknesses (300 microns).

AMO measurements showed no significant differences between test and control samples. However this time a slight advantage was observed for the gettered cells, although the difference was within the sample error limit. The  $I_{sc}$  of the gettered cells was 104.3 mA compared to the  $I_{sc}$  of the control samples which was 103.8 mA. The  $V_{oc}$  was 585 ± 2 mV and 583 ± 3 mV for test and control cells respectively. The 850°C phosphorous gettered samples had higher currents than the 900°C phosphorous gettered samples, reflecting for the most part the thicker wafer size.

Spectral response measurements also show the 850°C gettered and control cells to be essentially equivalent, with a slight (2%) advantage in response at 1.05 microns observed for the gettered samples. This is in contrast to the 900°C gettered cells where the samples had lower long wavelength responses than the control cells.

Spectral response curves for the 850°C gettered samples are not included since the data is essentially indistinguishable from the controls.

Analysis of the results of the phosphorous gettering work indicate that no advantage has been obtained. If anything, the importance of maintaining moderate processing temperatures is felt to have been demonstrated. Whereas a 900°C getter might be expected to remove more impurities than a 50°C lower getter, cell characteristics indicate a modest advantage in cell output is affected through the use of the lower processing temperature. The potential advantage of a phosphorous getter can be at best considered slight with gains falling within experimental accuracy limits.

### 2.2.2 Aluminum Gettering

Following the phosphorous gettering work a group of wafers was obtained for aluminum gettering studies; half were retained as controls and the remainder coated with approximately 6  $\mu\text{m}$  of evaporated aluminum. The aluminized wafers were alloyed at 850°C for 40 minutes, the excess aluminum residue was removed, and all wafers including controls were etched down 150-200 microns in 30% NaOH. Again, to prevent the redeposition of impurities all wafers were subjected to a PNH cleaning, followed by a  $\text{PH}_3$  diffusion at 825°C, providing a sheet resistance of  $\sim 100$  ohms per square.

Cells were fabricated in the normal manner, and measurements obtained without AR coatings. Since the Al gettered wafers averaged 25 microns less in thickness their values were corrected to compare with the 260 micron thick controls. AMO  $I_{sc}$  and  $V_{oc}$ , at 25°C were:

	$I_{sc}$	$V_{oc}$
Controls	103 ± 2 mA	584 ± 6 mV
Aluminum Gettered	100 ± 3 mA	577 ± 9 mV

These data indicate a slight loss for the gettered cells, similar to the work on  $PH_3$  gettering, although all values are comparable within the experimental limits. A spectral response analysis indicated that the current difference resided in the medium and long wavelength regions. (Figure 4)

Following these initial results a second and similar evaporated Al getter was performed at 850°C, since spectral response measurements of the first evaporated Al getter samples had indicated a severe loss in mid and long wavelength spectral response (see Figure 4) indicative of material lifetime degradation. The loss in response at 1.05 microns was approximately 35% with a nearly 20% loss evident at .9 microns. These values were quite in contrast to the smaller variations observed for  $PH_3$  gettering. For this reason it was felt that it would be worthwhile repeating this experiment and an additional 8 controls and 8 samples were subjected to the same process. In this repeat test all cells were measured for electrical performance and spectral response, and no significant differences were observed between controls and gettered samples. At the same time it was not possible to identify any possible differences in the processing used for the first group of cells tested previously. It was noted that even after 30-70 microns have been removed from each side of the Al gettered wafers, the gettered wafers can be identified from the controls by the appearance of bumps

and pockets due to etching the uneven surface produced by the aluminum alloying. This might indicate the possibility of residual stresses in the silicon surface which might account for lifetime losses. However the validity of this was greatly compromised by the fact that the second group of Al cells, which did not show any loss in lifetime, exhibited a significantly more eroded surface than the first group, which had the larger degradation. Although a specific degradation mechanism (introduction of impurities or stresses) cannot be defined by the limited data it is interesting to propose that the performance of evaporated aluminum BSF cells may be compromised due to the introduction of lifetime degradation by the BSF process.

A third experiment was then conducted using a paste Al BSF process which has been very successful in cell fabrication. This tended to further indicate that the evaporated Al process can cause lifetime degradation. In this experiment Al paste was applied to a surface of the sample wafers and after drying, heated to 900°C for 20 minutes. The wafers were then etched in 30% NaOH to remove approximately 70 microns of silicon from each surface, PNH cleaned and fabricated into solar cells as before. The material for these samples was of slightly lower resistivity (1½ vs. 2 ohm-cm) than used with the evaporated Al cells, but this was not felt to be significant.

AMO measurements showed the following characteristics:

	$I_{sc}$ (mA)	$V_{oc}$ (mV)
Al paste getter	102.3 ± 0.8	590 ± 3
controls	102.5 ± 1.3	587 ± 1

The equivalency of output was reflected in the spectral response where no significant difference could be noted in any wavelength band from .4-1.05 microns. At this point the aluminum getter work indicated (1) that no significant gettering enhancement had occurred, (2) that the higher temperature Al paste getter did not reduce bulk lifetime, and (3) that lifetime degradation may occur in the evaporated aluminum getter process.

Of all the gettering approaches the Al paste process appeared to hold the greatest promise.

Consequently, a limited amount of 0.5 ohm-cm silicon material was made available for additional analysis of gettering. It was felt that the lower resistivity might exaggerate any gettering impact compared to the lower doped 2 ohm-cm material. Following the application and drying of the paste, the wafers were heated at 900°C for twenty minutes. It was noted that a number of wafers had regions of spalling due to the thermal expansion coefficient mismatch of the aluminum paste and the silicon which is apparently aggravated by the long heating cycle. Since the aluminum residue and approximately three mils of silicon were to be removed from the wafer surface in a hydroxide etch it was not known if the spalling would cause any cell problems. Hence all samples were prepared for diffusions and processed into cells. As it turned out no significant electrical differences were noted between the spalled and the non-spalled gettered samples, although the silicon thickness through the spalled region was approximately 25 microns less. Comparison to non-gettered 0.5 ohm-cm controls is shown below.

	$I_{sc}$ (mA)	$V_{oc}$ (mV)
gettered	104.5 ± 1.0	583 ± 7
control	103.1 ± 0.3	592 ± 3

As in previous tests, cell characteristics are for non-AR coated cells. The gain in  $I_{sc}$  for the gettered cells is 1.2% and although slight does appear real. The current gain is offset by a 1.5% loss in  $V_{oc}$ , which may be due to processing problems, since there is a large variation in the data. Spectral response data were obtained in order to characterize the nature of the current increase in the gettered samples. Figure 5 shows average spectral response for the gettered and control cells. Consistent with a gettering benefit to lifetime is a higher long wavelength response in the aluminum gettered cells, with a 7.5% gain at 0.95 microns.

These results were felt to indicate that the gettering process might be of some benefit to the lower resistivity material, although at present gains are quite minimal. In order to explore the process potential further alternate gettering temperatures were examined. It is desirable to minimize high temperature excursions in cell fabrication since this lessens the possibility for lifetime damage; however, the removal of impurities by gettering is contingent on the mobility of the impurities in silicon which usually suggests that higher temperatures may be more practical.

For this reason three groups of wafers with aluminum paste were gettered at  $800^{\circ}\text{C}$ ,  $850^{\circ}\text{C}$ , and  $900^{\circ}\text{C}$  for 20 minutes. This range was chosen to extend the range examined previously, and to comply with the reasonable temperature limits.

All wafers were nominal 1 ohm-cm silicon. Following the gettering the alloyed aluminum region was removed by hydroxide etching, along with approximately 70 microns of silicon from each side. Final wafer thickness was approximately 275 microns. A group of control wafers were etched down along with the gettered wafers, and all groups were fabricated together, in order to minimize fabrication variations.

Electrical results are shown in Table 2, this time for Ta<sub>2</sub>O<sub>5</sub> AR coated samples.

TABLE 2  
GETTERED CELL ELECTRICAL PERFORMANCE

Cell Type	I <sub>sc</sub> (mA)*	V <sub>oc</sub> (mV)	I <sub>e</sub> 500 mV (mA)
800°C getter	131.4 ± 2.4	600 ± 2	123.4 ± 2.9
850°C getter	135.4 ± 1.2	602 ± 1	127.9 ± 2.2
900°C getter	135 ± 1	602 ± 1	127.8 ± 1.5
controls	134.7 ± 1.6	602 ± 1	127.7 ± 1.4

\*Approximately 8 wafers of each type

With the exception of the 800°C samples, all groups are equal. This is not too unexpected since it was proposed earlier that gettering would be more beneficial for lower resistivity material and since an approximate advantage of one percent had been noted for 0.5 ohm bulk silicon the lesser benefit on 1 ohm is reasonable. The surprise is the performance of the 800°C getter samples which are appreciably lower than all other groups. Spectral response measurements show the loss to be in the mid and long wave-regions. Since the aluminum paste used for gettering has been employed successfully for a BSF at the 800°C temperature it is difficult to ascribe any specific mechanism to this anomaly. And since all wafers were processed together there is no reason to select any other step as the cause of the loss.

Possibly a significant quantity of impurities were collected toward the aluminum but were still 2-3 mils from it after the heating. They might then remain within the bulk near the back surface after silicon etching to degrade the cell output.

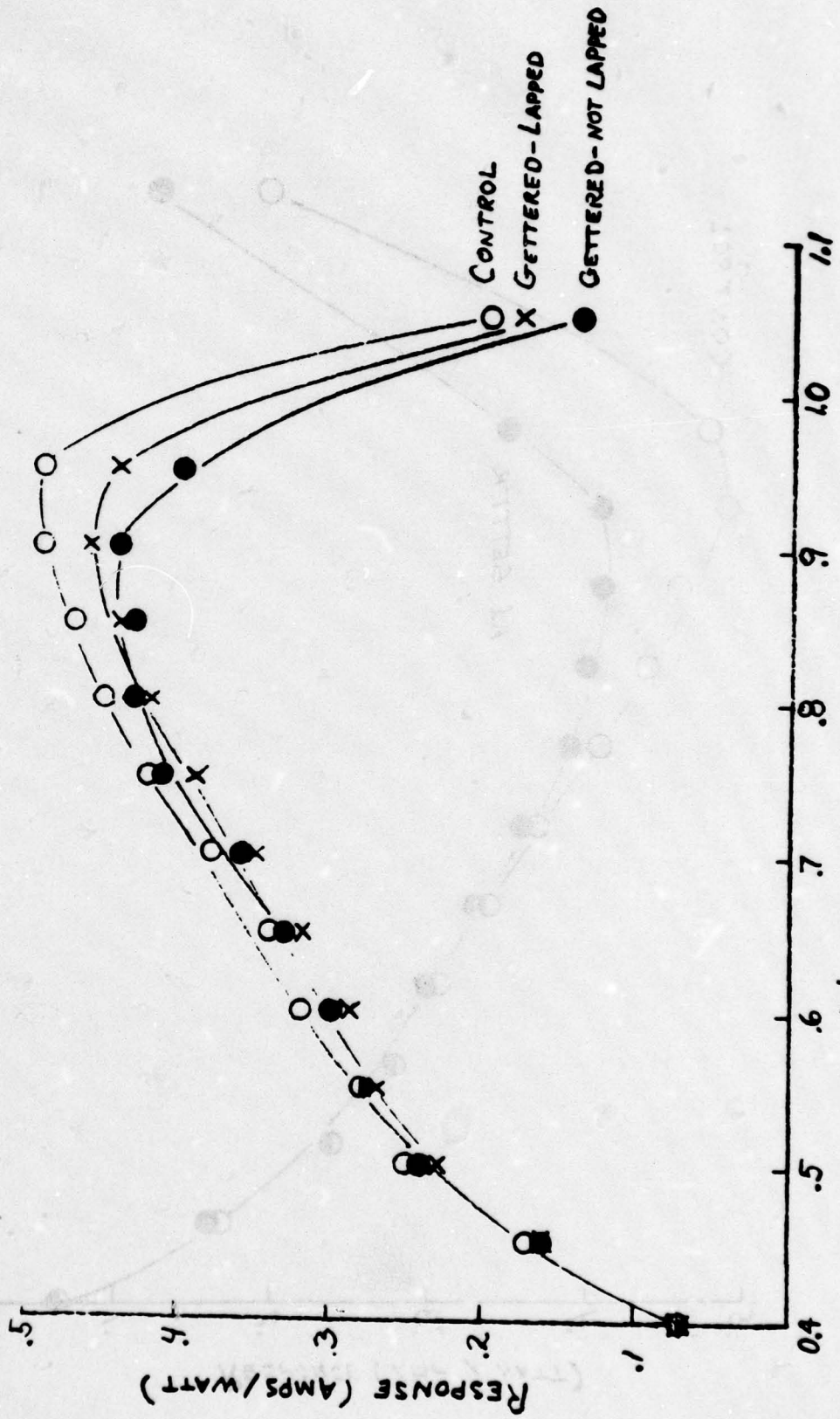


Figure 3 Spectral Response - Phosphorous Getter (900°C)

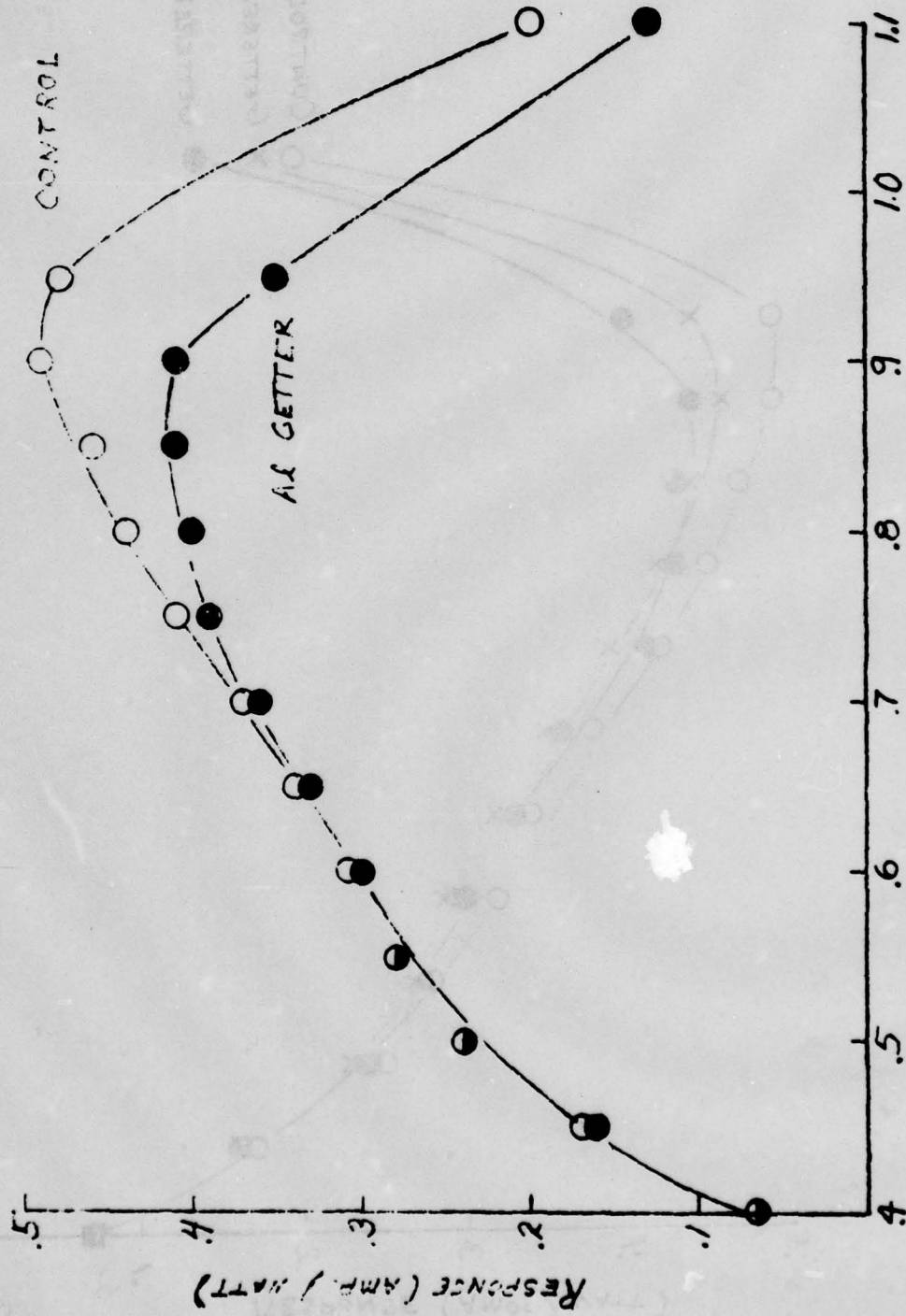


Figure 4 Spectral Response - Al (Evap.) Getter

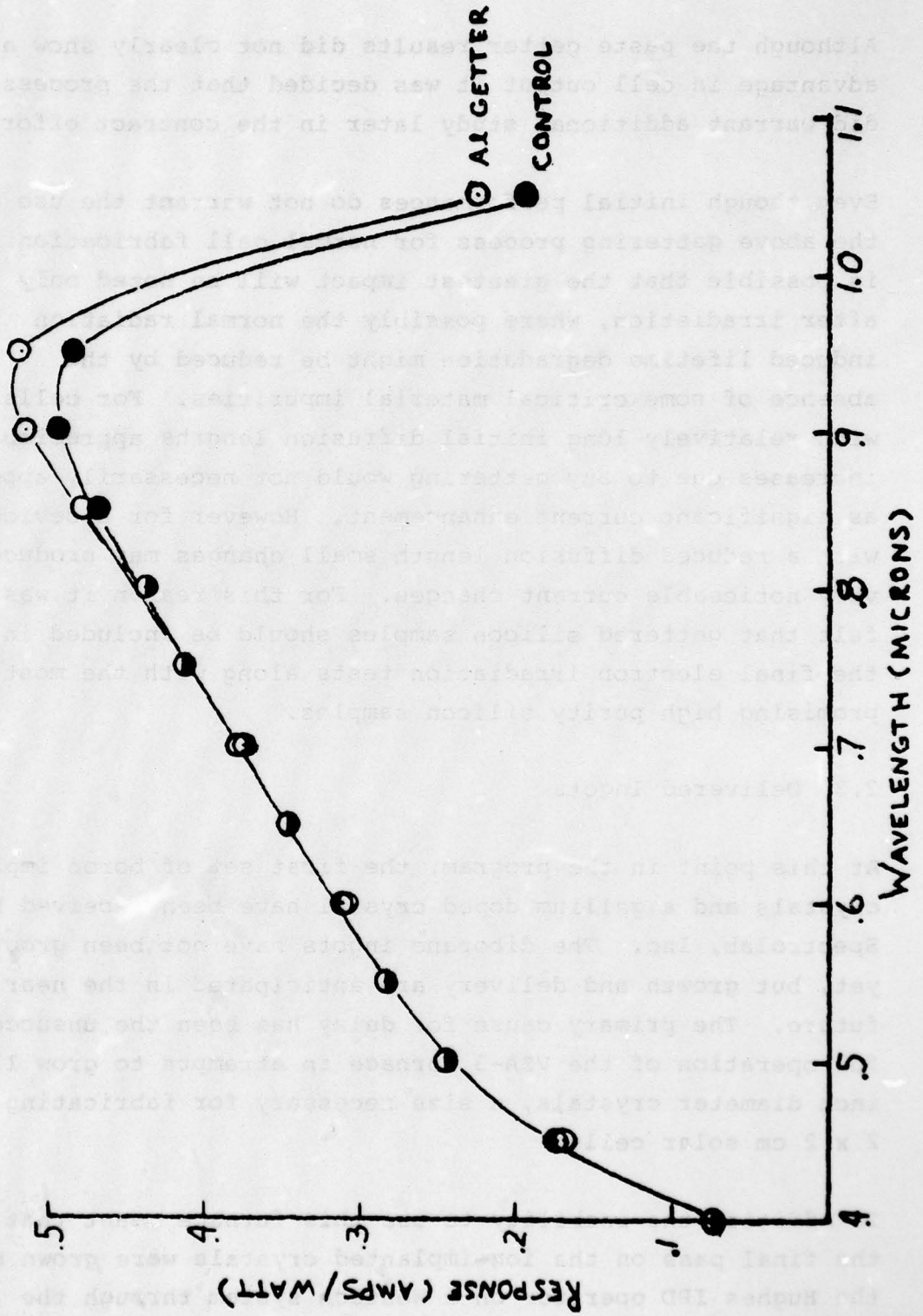


Figure 5 Spectral Response - Al Getter (.05 ohm-cm silicon)

Although the paste getter results did not clearly show an advantage in cell output it was decided that the process did warrant additional study later in the contract effort.

Even though initial performances do not warrant the use of the above gettering process for normal cell fabrication it is possible that the greatest impact will be noted only after irradiation, where possibly the normal radiation induced lifetime degradation might be reduced by the absence of some critical material impurities. For cells with relatively long initial diffusion lengths appreciable increases due to any gettering would not necessarily appear as significant current enhancement. However for a device with a reduced diffusion length small changes may produce very noticeable current changes. For this reason it was felt that gettered silicon samples should be included in the final electron irradiation tests along with the most promising high purity silicon samples.

### 2.3 Delivered Ingots

At this point in the program, the first set of boron implanted crystals and a gallium doped crystal have been received by Spectrolab, Inc. The diborane ingots have not been grown yet, but growth and delivery are anticipated in the near future. The primary cause for delay has been the unsuccessful operation of the VZA-3 furnace in attempts to grow 1.25 inch diameter crystals, a size necessary for fabricating 2 x 2 cm solar cells.

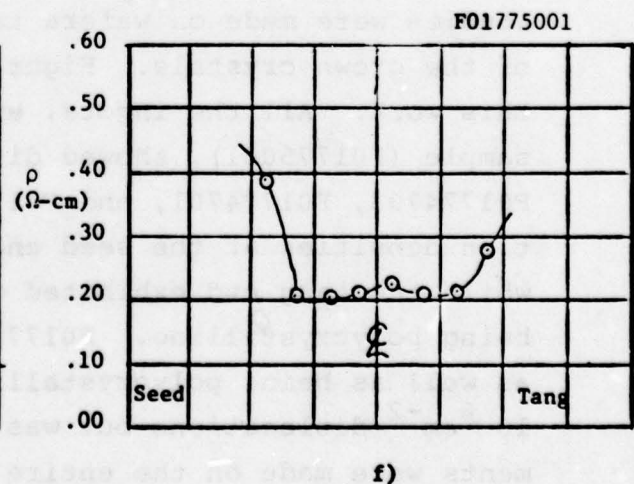
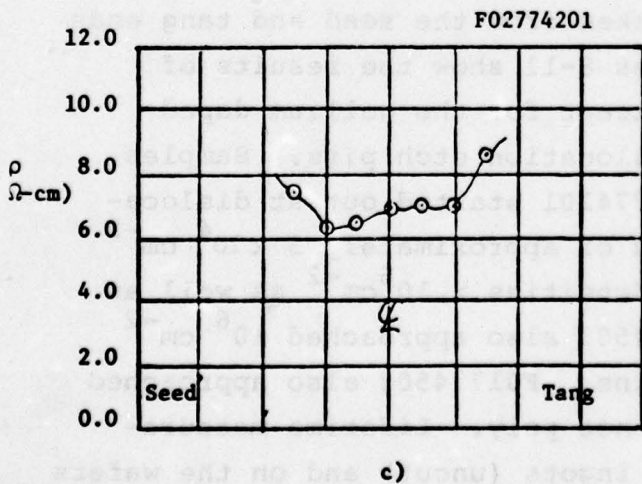
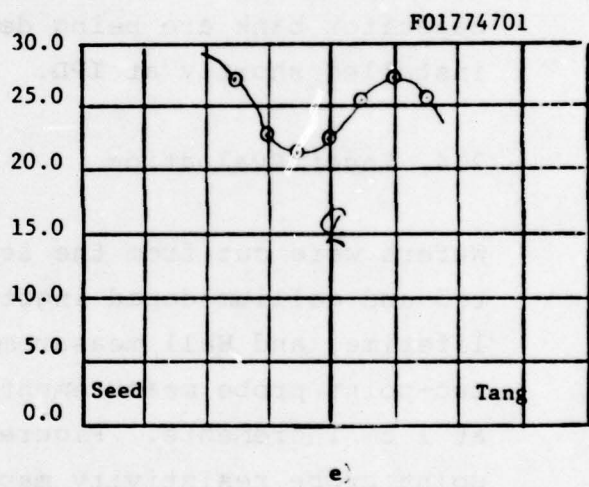
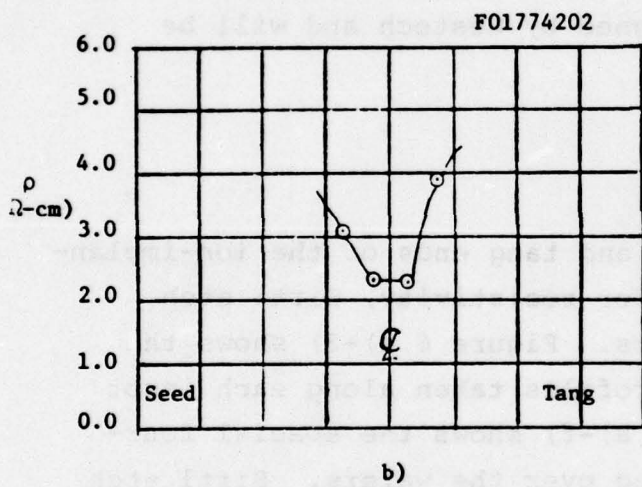
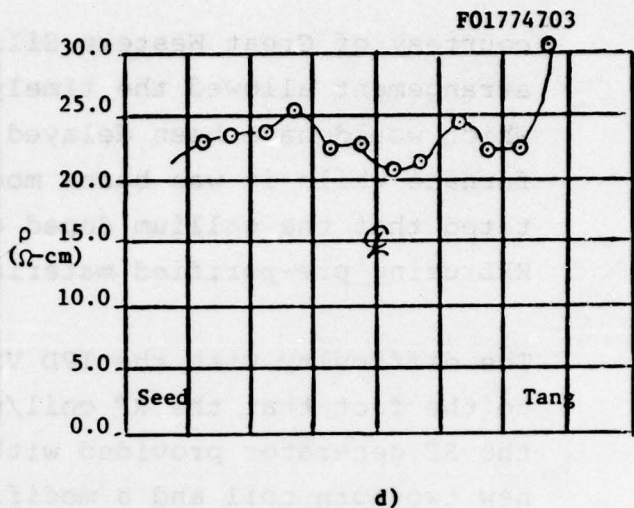
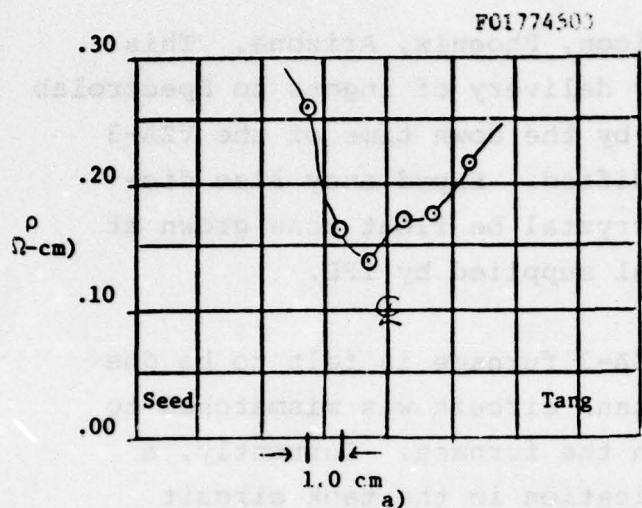
In addition the inability to use this furnace meant that the final pass on the ion-implanted crystals were grown by the Hughes IPD operator on a Westech system through the

courtesy of Great Western Silicon, Phoenix, Arizona. This arrangement allowed the timely delivery of ingots to Spectrolab which would have been delayed by the down time of the VZA-3 furnace while it was being modified. Expediency also dictated that the gallium doped crystal be float zone grown at HRL using pre-purified material supplied by IPD.

The difficulty with the IPD VZA-3 furnace is felt to be due to the fact that the RF coil/tank circuit was mismatched to the RF generator provided with the furnace. Currently, a new two-turn coil and a modification in the tank circuit capacitor bank are being designed by Westech and will be installed shortly at IPD.

#### 2.4 Ingot Evaluation

Wafers were cut from the seed and tang ends of the ion-implanted and gallium doped ingots for resistivity, Sirtl etch, lifetime, and Hall measurements. Figure 6 a)-3) shows the two-point probe measurement profiles taken along each ingot at 1 cm increments. Figure 7 a)-f) shows the spacial four-point probe resistivity mapping over the wafers. Sirtl etch studies were made on wafers taken from the seed and tang ends of the grown crystals. Figures 8-11 show the results of this work. All the ingots, except for the gallium doped sample (F01775001), showed dislocation etch pits. Samples F01774703, F01774701, and F01774201 started out at dislocation densities at the seed end of approximately  $3 \times 10^4 \text{ cm}^{-2}$  while the tang end exhibited densities  $> 10^6 \text{ cm}^{-2}$  as well as being polycrystalline. F01774503 also approached  $10^6 \text{ cm}^{-2}$  as well as being polycrystalline. F01774503 also approached  $10^6 \text{ cm}^{-2}$  dislocations but was not poly. Lifetime measurements were made on the entire ingots (uncut) and on the wafers from both the seed and tang ends using a Westech Lifetime

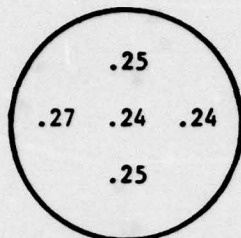


2-point probe measurements along length of ingot. 1 cm spacing between data points.

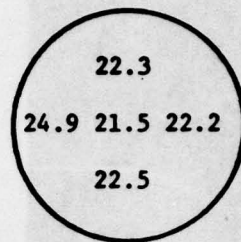


Seed

a) F01774503

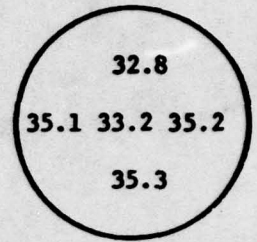


Tang

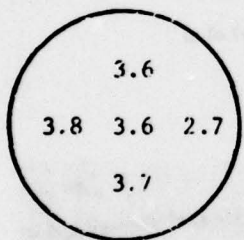


Seed

d) F01774703

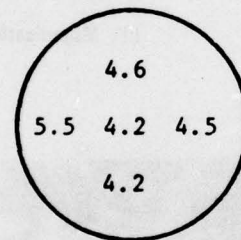


Tang

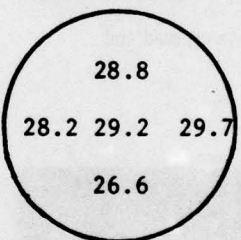


Seed

b) F01774202

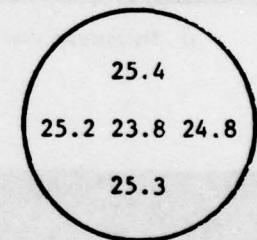


Tang

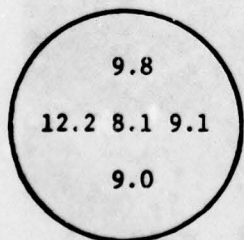


Seed

e) F01774701

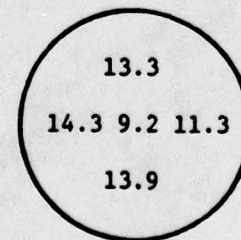


Tang

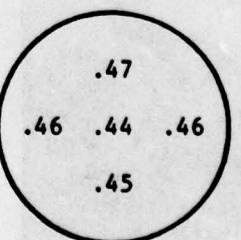


Seed

c) F02774201

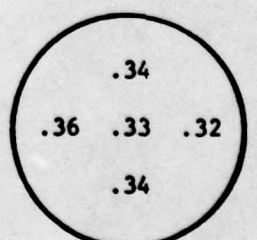


Tang



Seed

f) F01775001

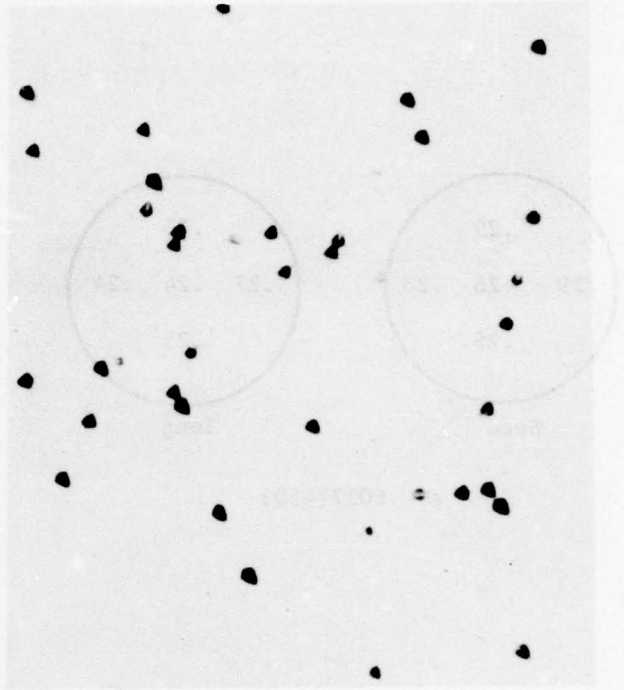


Tang

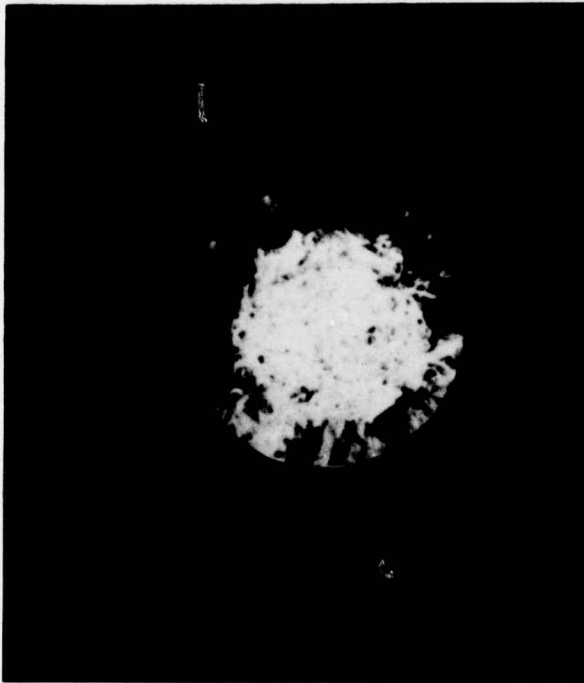
Figure 7 4-point probe measurements ( $\Omega$ -cm) in spacial 5 position pattern on seed and tang end wafer samples



a) Macroscopic view of etched wafer, seed end



b) Magnification (200x) of a)



c) Macroscopic view of etched wafer, tang end

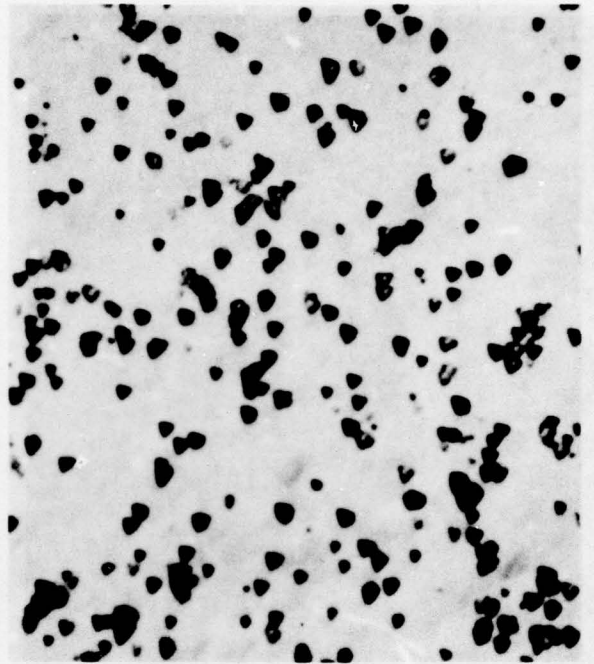


d) Magnification (200x) of c)

Figure 8 Sirtl etch pattern of ingot #F01774703 (20  $\Omega$  cm, boron)



a) Macroscopic view of etched wafer, seed end



b) Magnification (200x) of a)



c) Macroscopic view of etched wafer, tang end

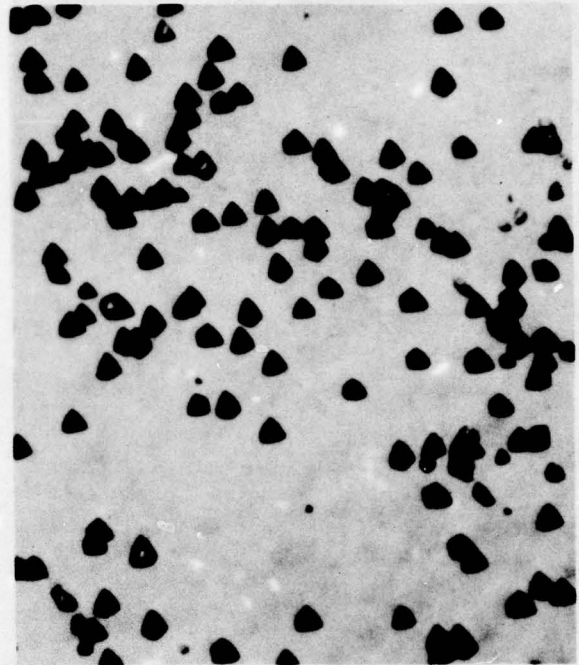


d) Magnification (200x) of c)

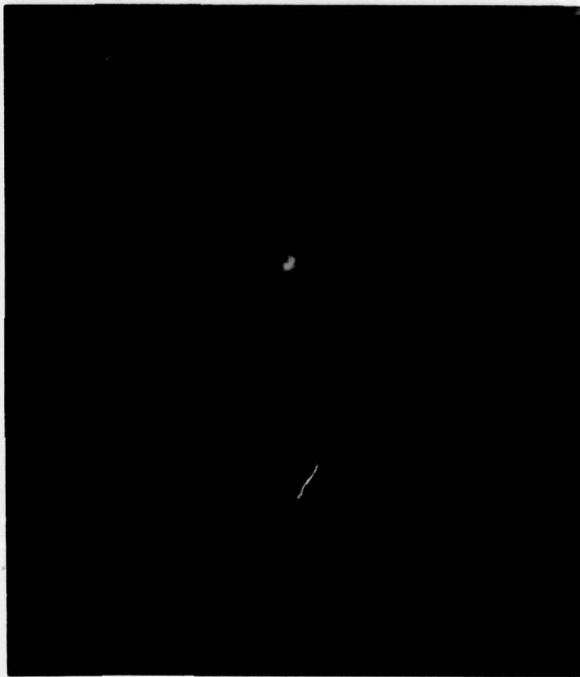
Figure 9 Sirtl etch pattern of ingot #F01774701 (20  $\Omega$  cm, boron)



a) Macroscopic view of etched wafer, seed end



b) Magnification (200x) of a)

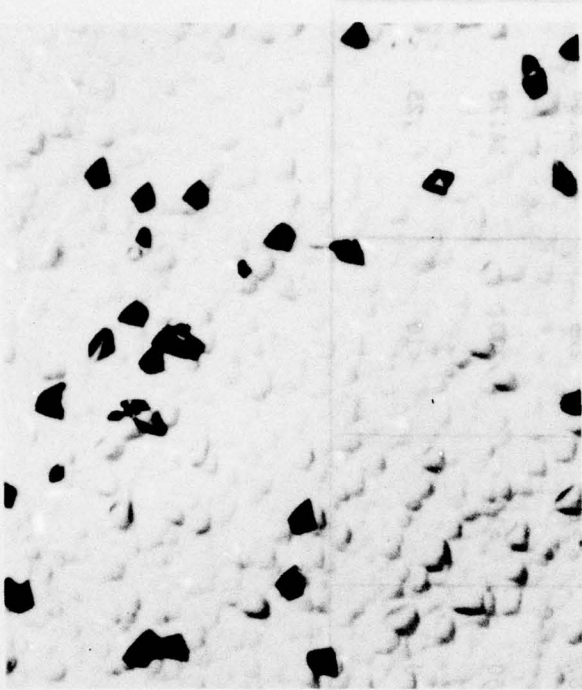


c) Macroscopic view of etched wafer, tang end

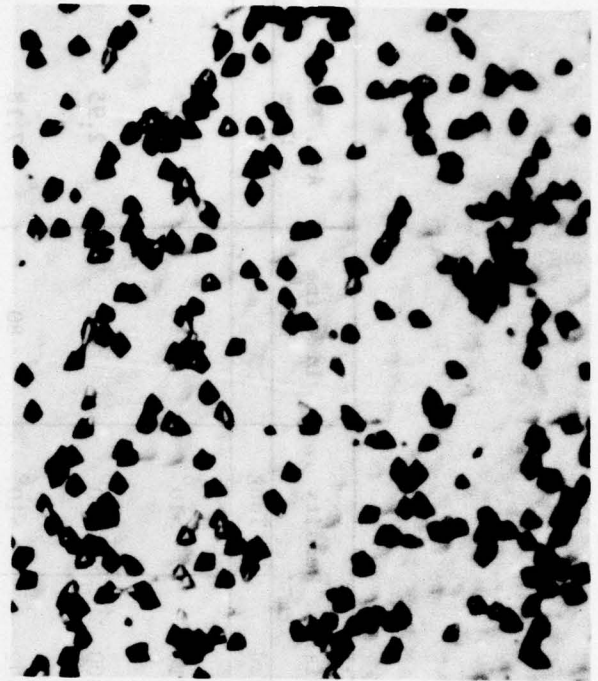


d) Magnification (200x) of c)

Figure 10 Sirtl etch pattern of ingot #F02774201 (7  $\Omega$  cm, boron)

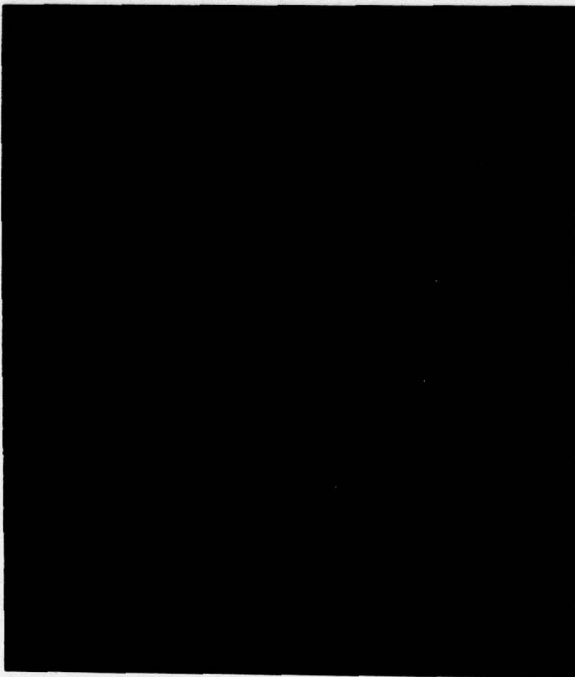


a) Magnification (200x) of seed end

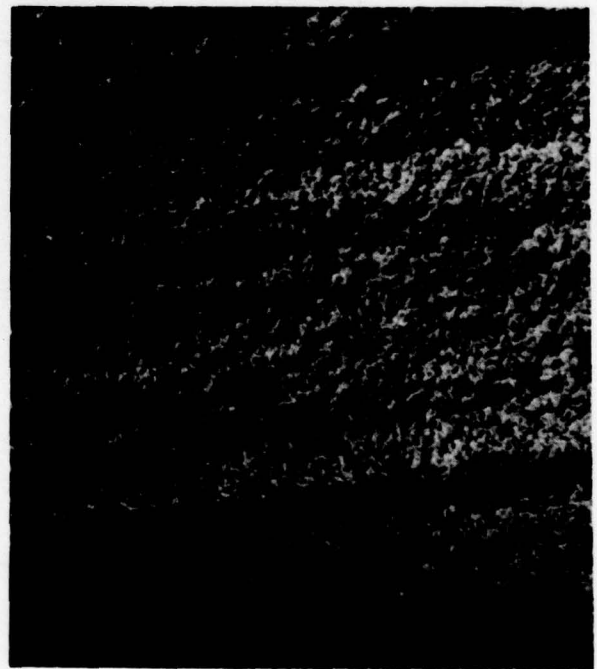


b) Magnification (200x) of tang end

Figure 11 Sirtl etch patterns of ingot #F01774503 (0.2  $\Omega$  cm, boron)



a) Macroscopic view of etched wafer, seed end



b) Magnification (50x) of tang end

Figure 12 Sirtl etch patterns of ingot #F01775001 (0.2  $\Omega$  cm, gallium)

TABLE 3  
INGOT CHARACTERISTICS

Crystal #	Useable Length cm	Nominal Dia. cm	Weight gm	Disloc. Density cm <sup>-2</sup>		Lifetime μs	Ave. Resis. Ω-cm
				Seed	Tang		
F01774503	4.58	3.26	86.1	38,718	>10 <sup>6</sup>	<10	.19
F01774202	4.15	3.21	77.8	232,000	>10 <sup>6</sup>	100	2.95
F02774201	5.89	3.20	109.3	37,602	>10 <sup>6</sup>	80	7.18
F01774703	10.99	2.94	170.2	18,987	>10 <sup>6</sup>	225	23.64
F01774701	6.00	3.04	99.2	27,550	>10 <sup>6</sup>	200	24.78
F01775001	10.55	3.36	221.2	0	0	<10	.25

Measurement system. A summary of the ingot grown length, supplied usable length, nominal diameter, weight, dislocation count, measured lifetime and average resistivity (two-point probe) are shown in Table 3.

Hall samples have been prepared and evaluated at HRL for room temperature and low temperature mobility runs in order to verify the purity of the ingot material. Table 1 summarizes the net dopant and net donor concentration results. There appears to be nothing unexpected in these results.

### 2.5 Cell Evaluation

All ingots were sliced into wafers of approximately 470 microns thickness. A portion of the wafers were selected from each ingot group and polish etched to a final thickness of 300 microns in order to remove all saw damage prior to cell fabrication. In addition a sample of as-sawn wafers were measured with a four-point probe for resistivity. In some cases differences were noted between initial ingot resistivity measurements and wafer measurements. Data are furnished below.

Ingot	Dopant	Desired	Ingot Value	Ave.
				Wafer Value
4701	Boron implant	20 ohm-cm	24.80 ohm-cm	not sliced
4703	Boron implant	20	23.60	25.5
4201	BF <sub>2</sub> implant	2	7.20	7.2
4202	Boron implant	2	2.90	2.3
4503	Boron implant	0.2	0.19	0.11
5001	Gallium	0.2	0.25	0.17

As shown above, data furnished with the ingots indicated very high dislocation counts for the boron and  $\text{BF}_2$  implanted ingots with values typically ranging from  $10^4/\text{cm}^2$  at the seed end to  $> 10^6/\text{cm}^2$  at the tang end. This was felt to be due to the use of a single zone pass after implantation.

The material degradation due to the dislocations is considered to be quite severe and in the case of the 20 ohm-cm ingot 4703, visual examination of the as-sawn wafers showed regions of polycrystallinity beginning within centimeters from the seed end and increasing in extent and size toward the tang end. Resistivity measurements showed the wafers toward the tang end to read 20% lower than the seed end. When this was noticed the remaining 20 ohm-cm ingot was held out from slicing since examination of the end caps showed the same type of pattern.

The ability to provide ingots with resistivities close to a desired value has been demonstrated with the boron implant and gallium doped ingots with the largest error noted in the 0.2 ohm-cm ingot which was measured at 0.11 ohm-cm. By contrast the  $\text{BF}_2$  implanted ingot fell well off the desired value. At this time no definite reasons have been given for this although it would appear that either the implant dosage was off or that an unexpectedly large fraction of the  $\text{BF}_2$  implant remained electrically inactive. Due to the unexpected resistivity value a number of as-sawn  $\text{BF}_2$  implanted wafers was heated at  $850^\circ\text{C}$  for two hours and then slow-cooled to  $400^\circ\text{C}$  in order to see if the resistivity would be thermally stable during normal processing situations. Before and after measurements showed no change in resistivity.

Following this, eight polished wafers were processed from each sliced ingot into 2 x 2 cm cells. For the boron implant wafers, material was selected nearer the seed end of the ingot in order to minimize any influence of the dislocations. Prior to diffusion all were thoroughly cleaned in a PNH process to remove metallic residues from the etching. Four 2 ohm-cm crucible grown wafers were included along with each group as controls. The finished cells were 300 microns thick with shallow phosphorus diffusions ( $\rho_s \approx 100$  ohms/square), polished surfaces, and no back surface fields. An N collector structure with twenty-four one mil (nominal) wide titanium-silver grids was evaporated onto the cells after sintering the rear Ag-Ti picture frame contact. Air mass zero output is shown below for all groups, without AR coatings, including all controls.

Cell Type	$I_{sc}$ (mA)	$V_{oc}$ (mV)
gallium-0.17 ohms	104.1	608
boron-0.1 ohm	99.5	593
boron-2.3 ohm	104.1	573
boron-7 ohm	105.5	558
boron-20 ohm	107.1	529
controls-2 ohm	106	588

Following the AMO, 25°C measurements, spectral response characteristics were obtained for all samples. This was undertaken in order to determine whether the current differences might be due to lifetime effects or other variables such as contact coverage or junction depth. Since the controls run with each group were quite consistent in output, processing variables were not felt to be suspect. The data presented below show the response relative to the 2 ohm-cm control cell response at a few pertinent wavelengths.

Cell Type	Relative Response				
	.45 $\mu$	.6 $\mu$	.8 $\mu$	.95 $\mu$	1.05 $\mu$
gallium	.95	.99	.98	.92	.88
0.1 ohm	.96	.98	.90	.74	.65
2.3 ohm	.96	.99	.99	1.01	1.07
20 ohm	.96	.99	.98	1.02	.95
7 ohm (not measured)					

Although the test samples are slightly lower at .45 $\mu$  than the controls, possibly due to contact coverage, the difference is small and does not impact the overall view. The lack of response in the long wavelength region shows the effect of the high dislocation density on the device lifetime. This is particularly evident in the 20 ohm-cm sample. The relatively equivalent response of the 2 ohm boron sample is tantalizing in that much high response might be anticipated with zero dislocation material. The gallium sample shows a relatively high long wavelength response when consideration is taken of the low resistivity of the material.

Final electrical performance measurements were then obtained after AR coating ( $Ta_2O_5$ ) and edge etching. Problems with rear contact indexing meant that due to metal over the cell edge, shunting might affect cell  $V_{OC}$  on the uncoated cells, so this data was especially important. Results are listed below.

Cell Type	$I_{sc}$ (mA)	$V_{oc}$ (mV)
gallium	146	627 (half of samples at 633 mV)
0.1 ohm boron	140	620
2.3 ohm boron	147	595
7 ohm boron	151	571
20 ohm boron	149	537
2 ohm controls	148	600

AMO I-V characteristics for typical cells in each group are shown in Figures 13 through 17. The control cell shown has a lower than anticipated FF but is typical in  $I_{sc}$  and  $V_{oc}$ . Since only a few control samples were AR coated the curve shape is not considered normal and values of .78 are more in line with past cell lots. However, reasonable comparisons between the  $I_{sc}$  and  $V_{oc}$  of all groups can be made and using .78 as a norm for the FF similar comparisons can be made.

The performance of the gallium samples stands out in the first comparison. The high  $V_{oc}$  and FF are achieved along with a very respectable  $I_{sc}$ , providing an AMO maximum power of 74.7 mW. By comparison the 0.1 boron implant group is deficient in all significant cell output parameters, especially  $I_{sc}$  and FF.

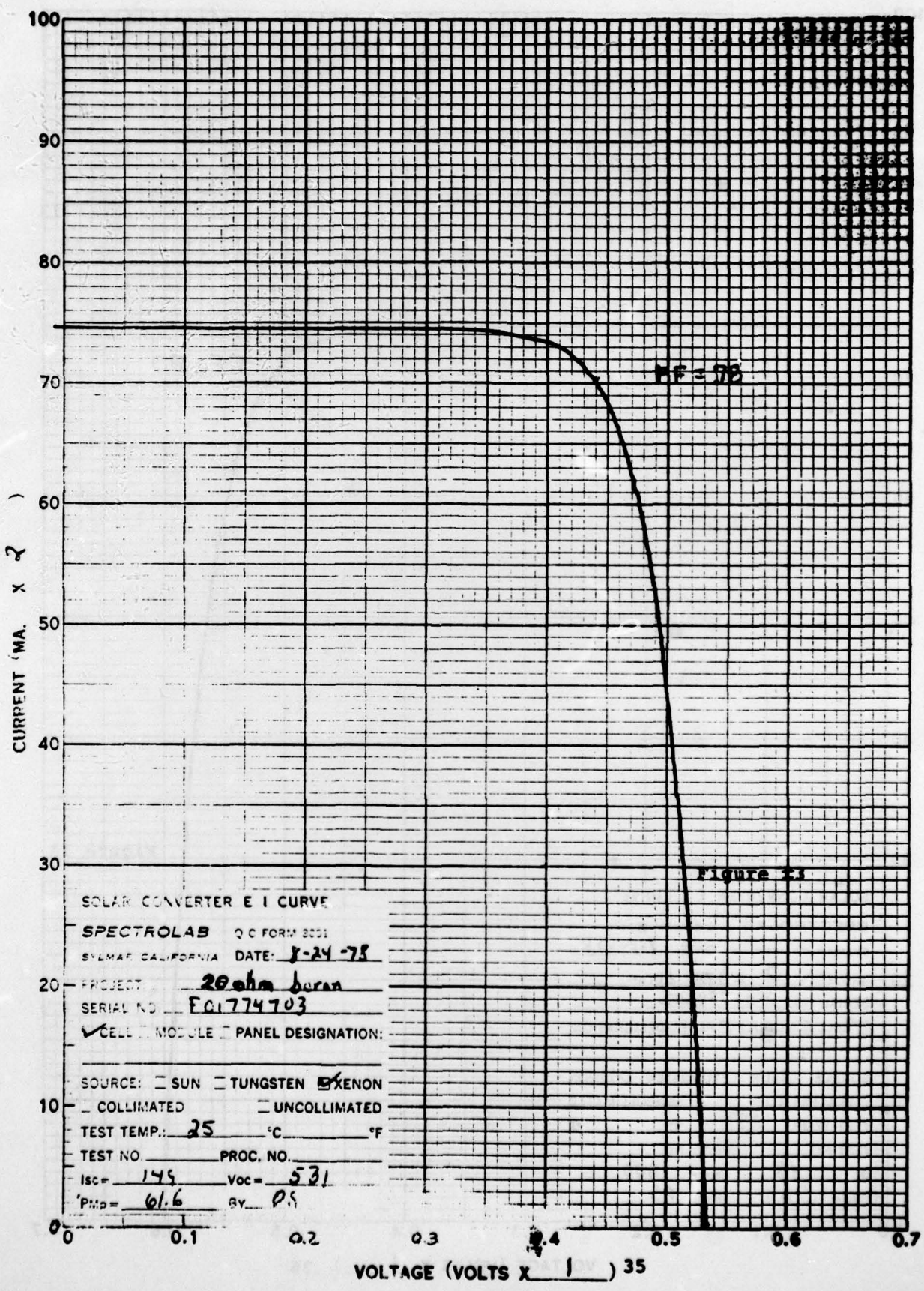
Similarly the 2 ohm controls and 2 ohm implant cells can make for an interesting comparison. Neglecting the FF, which may be due to slight shunting at an edge chip on the controls the implant cell exhibits lower  $I_{sc}$  and equivalent  $V_{oc}$ , not as might be expected.

Since it is felt that the high dislocation density may indicate structural problems which could reduce device performance it is instructive to examine the 20 ohm-cm implant cells. As mentioned above this ingot had the

severest visible crystal damage. Normally the  $I_{sc}$  of 20 ohm-cm material would be much higher than the lower resistivity materials, however in this case it is comparable to both 2 ohm controls and implant cells. It must be assumed from this that all implant samples are degraded an unknown amount by the material problems, with the greatest damage in the highest resistivity (lowest doping level). Although the extent of the output loss cannot be quantified for each cell group it is significant to note that visual (unaided eye) examination of the implant cells can reveal occasional lattice damage in the form of lineage, ranging from none to one to many per cell.

Of all the samples, the gallium doped silicon results are the most encouraging. A valid evaluation of the boron implant samples cannot be made unless the ingot crystal can either be made with substantially lower dislocations or until it is shown that the implant technique incurs crystallinity defects.

Regardless of the boron implant outcome, at this time, the gallium cells show promise of a potential breakthrough in achievable cell characteristics. Although the 633 mV output is the highest observed at Spectrolab on a non-BSF cell, improvements in cell output brought about by additional advanced cell processing (which would possibly require a change in material crystal orientation) could through increased  $I_{sc}$  and a BSF addition, provide over 640 mV. Although the BSF  $V_{oc}$  enhancement is reduced for lower resistivities, a gain of 25 mV on 2 ohm-cm material suggests that 0.2 ohm-cm material may still pick up from 5 to 10 mV. And with improved  $I_{sc}$ , due to reflection reduction on the front surface, and a BSF and BSR, an additional 5 mV could be realistically expected for a total  $V_{oc}$  of 643 to 648 mV.



SOLAR CONVERTER E I CURVE

SPECTROLAB Q.C. FORM 8001

SYLMAR, CALIFORNIA DATE: 8-24-75

PROJECT: 20 ohm buran

SERIAL NO. FG1774703

CELL  MODULE  PANEL DESIGNATION:

SOURCE:  SUN  TUNGSTEN  XENON

COLLIMATED  UNCOLLIMATED

TEST TEMP.: 25 °C \_\_\_\_\_ °F

TEST NO. \_\_\_\_\_ PROC. NO. \_\_\_\_\_

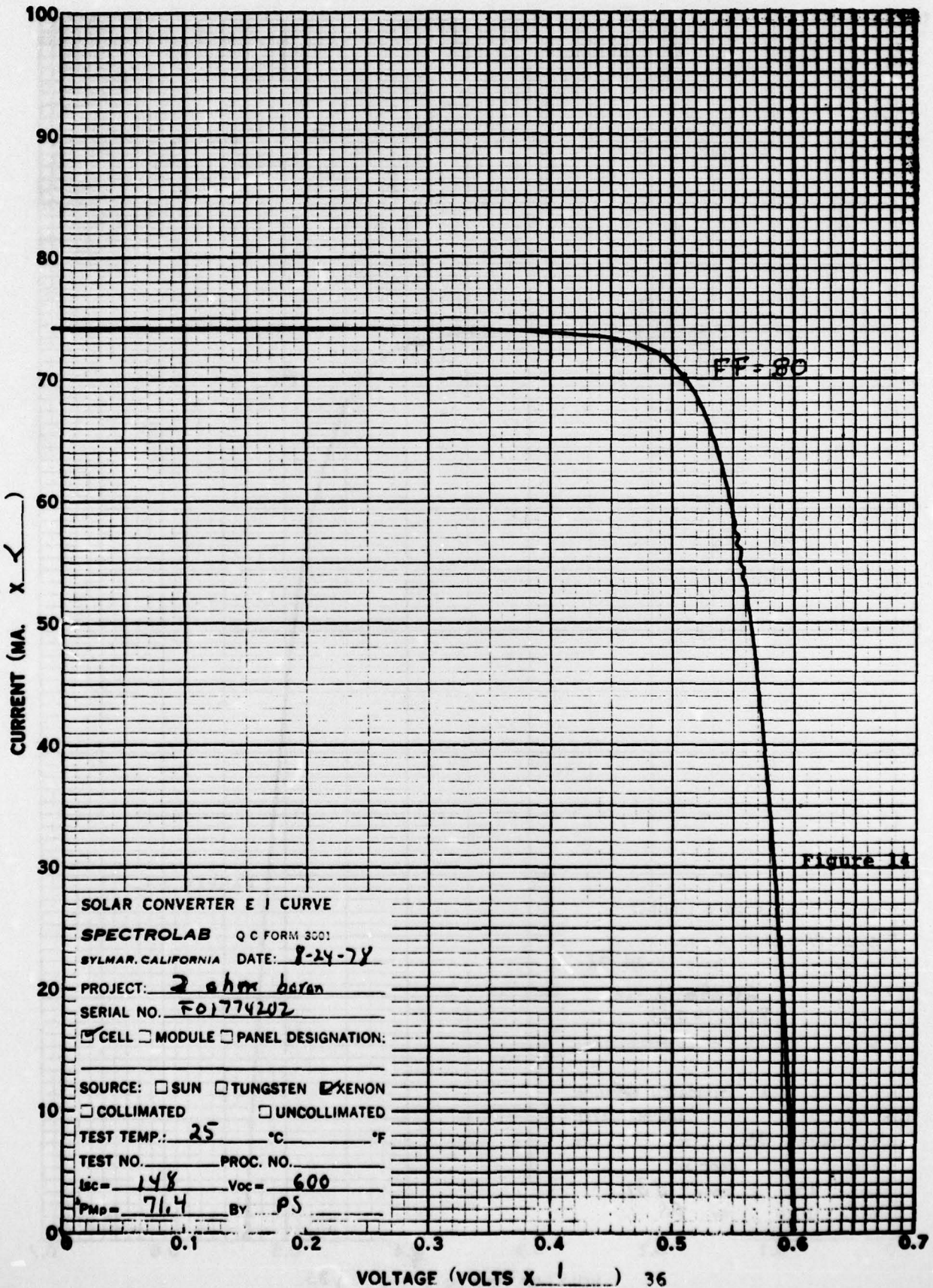
I<sub>sc</sub> = 145 Voc = 531

P<sub>mp</sub> = 61.6 BY: PS

FF = 78

Figure 13

VOLTAGE (VOLTS X 1) 35



SOLAR CONVERTER E I CURVE

SPECTROLAB Q C FORM 3001

SYLMAR, CALIFORNIA DATE: 8-24-78

PROJECT: 2 ohm baron

SERIAL NO. F01774202

CELL  MODULE  PANEL DESIGNATION:

SOURCE:  SUN  TUNGSTEN  XENON

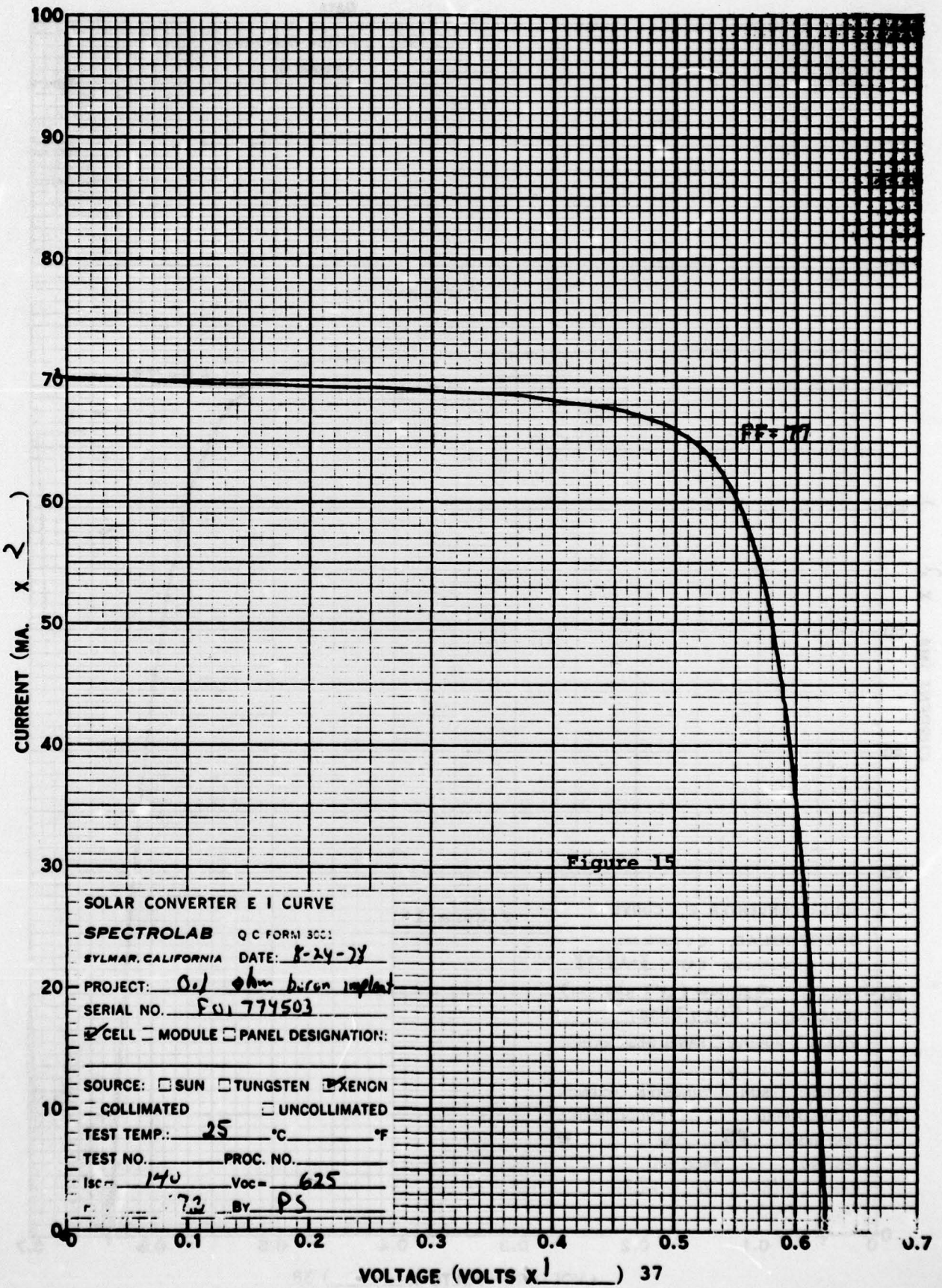
COLLIMATED  UNCOLLIMATED

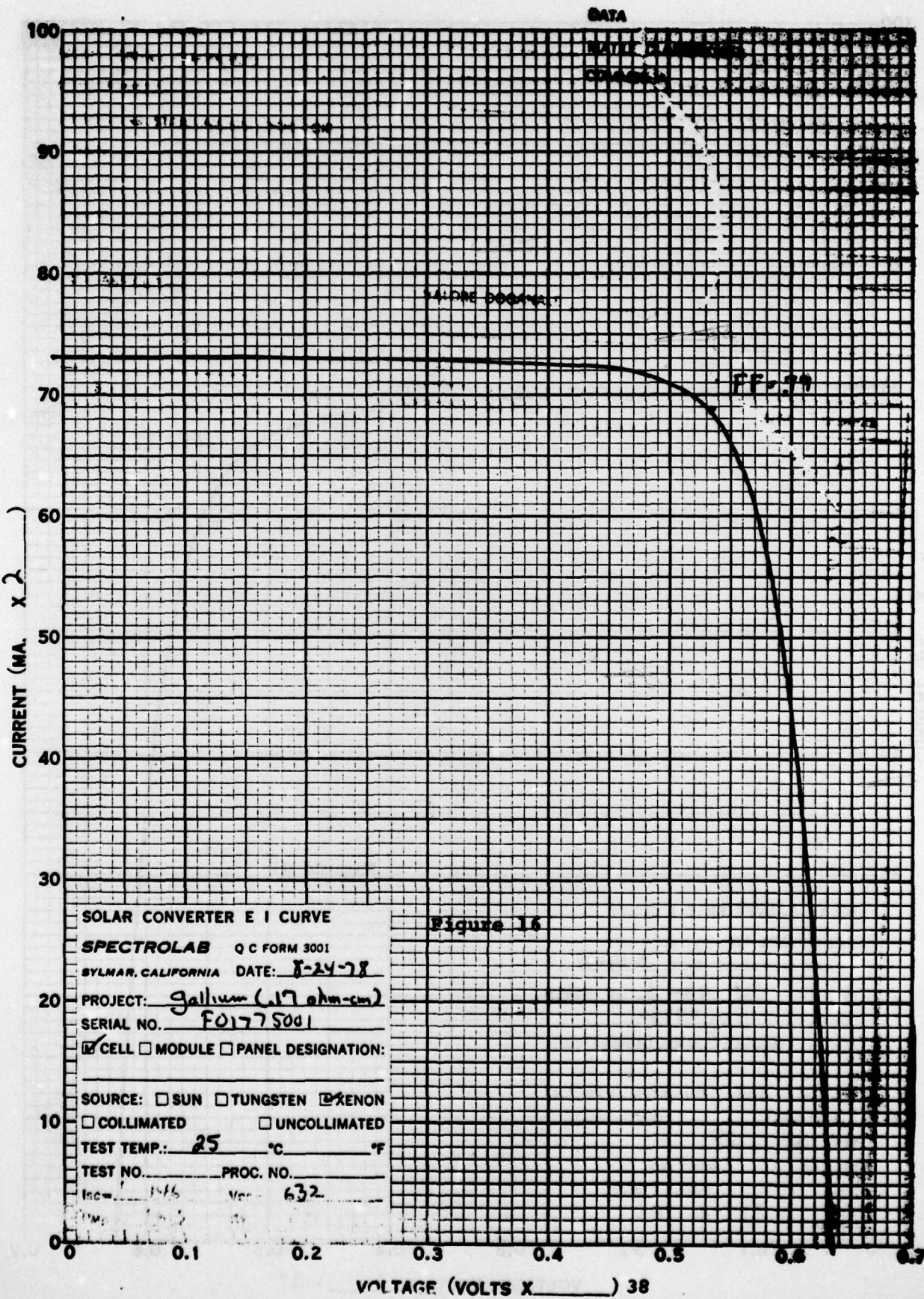
TEST TEMP.: 25 °C °F

TEST NO. PROC. NO.

Isc = 148 Voc = 600

PMP = 71.4 BY PS





**SOLAR CONVERTER E I CURVE**

**SPECTROLAB** Q C FORM 3001

BYLMAR, CALIFORNIA DATE: 8-24-78

PROJECT: Gallium (.17 ohm-cm)

SERIAL NO. F01775001

CELL  MODULE  PANEL DESIGNATION:

SOURCE:  SUN  TUNGSTEN  XENON

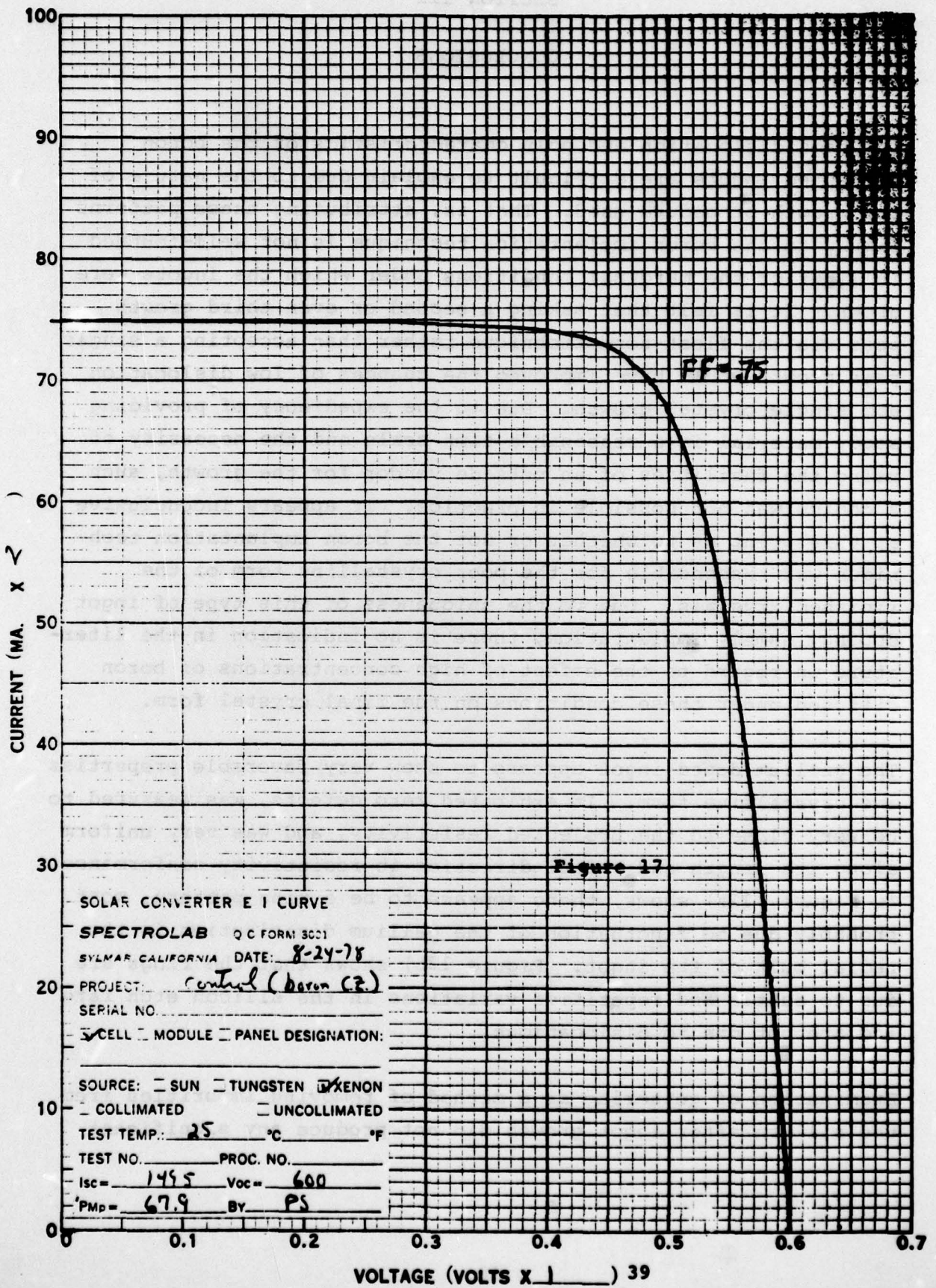
COLLIMATED  UNCOLLIMATED

TEST TEMP.: 25 °C \_\_\_\_\_ °F

TEST NO. \_\_\_\_\_ PROC. NO. \_\_\_\_\_

ISC = 146 V<sub>OC</sub> = 632

VOLTAGE (VOLTS X \_\_\_\_\_) 38



### SECTION III

#### CONCLUSIONS

The high dislocation and poly characteristics of the boron implanted ingots are difficult to explain due to the nature of the growth procedure used. That is, attributing these patterns simply to the boron implantation technique is not well-founded in light of the marginal conditions under which the ingots were grown. It is felt that making a second or even third growth pass via the float-zone technique rather than accepting a single pass growth would have improved the chances of low dislocation and single crystal growth. Due to the expediency of providing study material in a reasonable time scale and the necessity of using the facilities of an outside vendor for the growth, such a choice was not possible in practice. It appears inconclusive at this point as to whether or not the boron implantation technique was responsible for the poor crystalline form of the finished crystals. Due to the uniqueness of this type of ingot doping, namely implantation, there is no indication in the literature in regard to the effect of high concentrations of boron diffused under these conditions on the final crystal form.

The gallium doped ingot appears to show very favorable properties and crystalline form. It exhibited zero defects, was measured to be very close to the projected resistivity, and was very uniform along its length and radial direction in resistivity conformance. As Figure 12a) shows, there appears to be a ring pattern, most probably due to fluctuation of the gallium distribution in the radial bulk of the ingot. Figure 12b) shows that the rings are due to subtle and repetitive variations in the silicon etch rate and are not due to dislocations.

Examination of gettering as a method of removing impurities from the silicon after ingot growth did not produce any significant

improvement in cell performance. Of the three methods examined, phosphorous, evaporated aluminum, and aluminum paste, only the last produced cells consistently equal to or better than the control cells. Although initial Al paste gettered cells did not exhibit any benefits consistent with the additional processing, full evaluation will require an electron irradiation test in order to see if the gettering has improved the damage rate.

Cell evaluation of the IPD supplied ingot material produced results consistent with the ingot evaluation. None of the boron implant wafers performed better than the standard boron CZ grown control cells, and in the case of the 20 ohm-cm devices, significantly poorer results were obtained than had been anticipated. In view of the problem with dislocations and polycrystallinity this is not totally unreasonable.

In contrast the gallium doped ingot which was grown under better conditions produced a number of very good 0.2 ohm-cm cells providing some of the highest  $V_{oc}$  values noted to date, 633 mV, without any BSF. At the same time  $I_{sc}$  values were approximately 98% of the 2 ohm-cm control cells, quite respectable considering the order of magnitude greater doping concentration.

## SECTION IV

### RECOMMENDATIONS

1. That as soon as VZA-3 is operating suitable for 1.25" diameter ingot, two boron ion implant ingots with resistivities of 2 and 0.2 ohm-cm be grown using additional passes to determine if dislocations, etc., can be reduced; that cells be fabricated from this material.
2. That a quick look electron irradiation test be performed on cells presently available.
3. That gaseous boron doped ingots be made and cells fabricated from those ingots.
4. That additional Ga doped ingots be grown (20, 10, 2 and 0.2 ohm-cm) and fabricated into solar cells.
5. That consideration be given to incorporating into the program test and evaluation to assure that impurities are not being introduced into the materials during cell processing.

### References

1. B. A. MacIver, E. Greenstein, J. Electrochem. Soc.: Solid-State Science and Technology, February 1977, p. 273-275.
2. R. L. Meek, T. M. Buck, and C. F. Biggon, "Silicon Surface Contamination; Polishing and Cleaning," J. Electrochem. Soc. Volume 120, No. 9, p. 1241.
3. J. A. Scott-Monck, P. Stella, and J. Avery, "Development of Processing Procedures for Advanced Silicon Solar Cells," Final Report NASA CR-134740, Jan. 1975,
4. J. Scott-Monck and P. Stella, "Textured Surface Cell Performance Characteristics," 12th Photovoltaic Specialists Conference Record, p. 600, 1976.